17th World Conference on Earthquake Engineering, 17WCEE

Sendai, Japan - September 13th to 18th 2020

SEISMIC PERFORMANCE ASSESSMENT OF STEEL LIGHT-FRAME PORT WAREHOUSES DUE TO GROUND SHAKING AND LIQUEFACTION

S. Karafagka[(1)], S. Fotopoulou[(2)], A. Karatzetzou[(3)], G. Malliotakis[(4)], D. Pitilakis[(5)]

[(1)] *Dr, Aristotle University of Thessaloniki, stellak@civil.auth.gr*
[(2)] *Dr, Aristotle University of Thessaloniki, sfotopou@civil.auth.gr*
[(3)] *Dr, Aristotle University of Thessaloniki, akaratze@civil.auth.gr*
[(4)] *Civil engineer, Aristotle University of Thessaloniki, georgsiteia@gmail.com*
[(5)] *Associate professor, Aristotle University of Thessaloniki, dpitilakis@civil.auth.gr*

Abstract

The interruption of port structures functionality can have severe effects on the economy and on the social and environmental growth of the broader area. Soft alluvial deposits, usually susceptible to liquefaction, characterize the subsoil conditions of ports. Experience gained from recent strong seismic events has demonstrated that even moderate levels of earthquake intensity can cause liquefaction, leading potentially to induced soil settlements and lateral spreading, that may produce serious damage to port infrastructure and hence result to significant economic and societal losses. Warehouses, which are large space steel light-frame buildings (with or without masonry infills), constitute key components of a port system. Although progress has been made on the influence of ground shaking and soil liquefaction on the structural response of steel frame buildings, studies coupling both phenomena are very limited. The present paper outlines the seismic performance of port warehouses resting on liquefiable soils, by conducting two-dimensional nonlinear incremental dynamic analysis (IDA). We follow the direct one-step approach where the soil and the structure are modelled and analysed as a single system taking also into account the liquefaction effects. The earthquake demand is determined based on the selection of real earthquake records that cover a wide range of seismic input motions in terms of amplitude, frequency content and significant duration. The seismic input motion is applied to the base of the soil model (bedrock). The calculated structural demand in terms of maximum inter-story drift is adopted as representative damage measure (or engineering demand parameter - EDP). We consider various seismic intensity measures (IM) to correlate with structural deformation demand through nonlinear regression analysis in order to identify the most appropriate ones. The Peak Ground Velocity at bedrock (PGV_{rock}) is found to better describe the performance of these large space steel light-frame buildings on liquefiable soils. Moreover, a good correlation of both Permanent Ground Displacement at surface (PGD_{surf}) and maximum differential settlement at the foundation level with the selected EDP is shown. The results of this study (IM- EDP pairs) can be used as a basis for the seismic fragility assessment of these type of buildings due to ground shaking and soil liquefaction.

Keywords: soil-structure interaction; liquefaction; intensity measures; steel light-frame warehouse; port

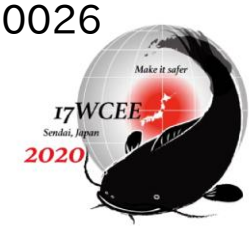

1. Introduction

Past seismic events in Greece (e.g. Lefkada M6.5 2003, Cephalonia M6.1 2014) and worldwide (e.g. Loma Prieta M6.9 1989, Hyogo-ken Nanbu (Kobe) M6.9 1995, Chi-Chi M7.3 1999, New Zealand M6.3 2011 and Tohoku, Japan M9.0 2011) have demonstrated the high vulnerability of port facilities to strong ground shaking and the induced phenomena, principally associated with liquefaction effects that often prevail at coastal areas [1-2], resulting to significant economic and societal losses [3]. Among the several components of a port, warehouses, which are large space steel light-frame buildings (with or without masonry infills), constitute key components of a port system [4]. Some progress has already been made on the influence of ground shaking and soil liquefaction on the structural response of steel frame buildings [5-6]. However, the published literature in the evaluation of the induced physical damages to steel frame buildings exposed to the combined effect of ground shaking and soil liquefaction is generally inadequate. In addition, most damage to coastal structures is the result of soil-structure interaction (SSI); hence, design and analysis procedures should include both geotechnical and structural conditions of coastal structures [3].

In this study we aim to assess the seismic performance of typical port steel light-frame warehouses resting on liquefiable soils considering soil-structure interaction (SSI). We implement the direct one-step approach where the soil and the structure are modelled and analysed as a single system, considering the potential for liquefaction. The seismic input motion is applied to the base of the soil model (bedrock). We conduct two-dimensional (2D) incremental dynamic analysis (IDA) to assess the performance of the steel light-frame warehouse on liquefiable soils. Three soft soil profiles susceptible to liquefaction are investigated. The warehouse's response is assessed in terms of maximum inter-story drift, which is the selected damage measure - engineering demand parameter (EDP). Different seismic intensity measures (IM) are statistically correlated with structural deformation demand (the selected EDP) through nonlinear regression analysis to finally identify the most appropriate ones. The outcome of this study (IM- EDP pairs) can be used as a basis for the seismic fragility assessment of these type of buildings due to ground shaking and soil liquefaction.

2. Numerical modelling

2.1 Selection of the reference building typology and soil profiles

In this study, we select a steel light-frame warehouse, representative of Thessaloniki port critical buildings, as reference structure for investigation of its seismic performance due to ground shaking and soil liquefaction. Fig. 1 illustrates a schematic view of the typical warehouse cross-section, as provided by the Port authorities. The main characteristics of the building, namely the total mass (m), the fundamental period (T) and the mean compressive strength of steel are set equal to m=5.1tn, T=0.30s and f_{ym}= 235.0 MPa respectively.

To compute the ground response, three representative soil profiles of the port area of Thessaloniki (Greece) are defined, simplified with respect to their total depth, denoted as SP1, SP2, and SP3 (Fig. 2), based on the available geotechnical information of the port area and the available SPT and laboratory data [7-8]. Their fundamental periods T_o are equal to 0.88 sec, 0.73 sec, and 0.64 sec, respectively. Fig. 2 presents the variation of the shear wave velocities V_S with the depth together with a general geotechnical characterization according to the USCS classification for the three soil profiles. The liquefaction potential of the subsoil layers of the selected soil profiles is quantitatively evaluated by following the guidelines of Eurocode 8 (EC8)- Part 5 [9]. For SP1 potentially liquefiable soil formations are found at depths z=-9÷-11m, z=-14÷-20m and z=-26.5÷-36m, for SP2 at depths z=-3÷-14m, while for SP3 at depths z=-4÷-20m, which are basically silty/clayey sands and non-plastic silts with low values of N_{SPT}. Thus, knowing that the liquefaction susceptibility in the port area is rather high, these soil profiles refer to ground type S according to EC8 classification.

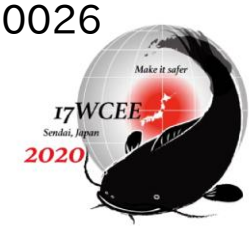

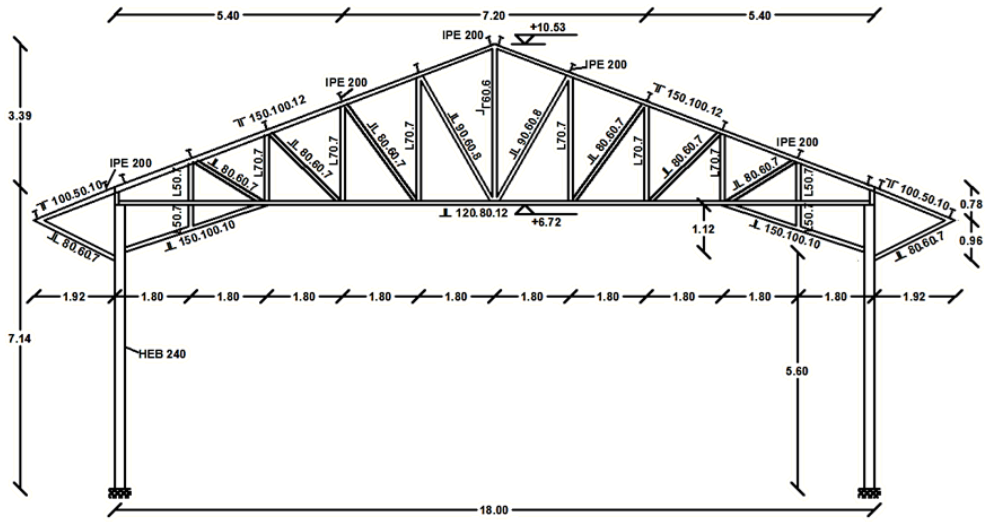

Fig. 1 – Cross-section of the warehouse

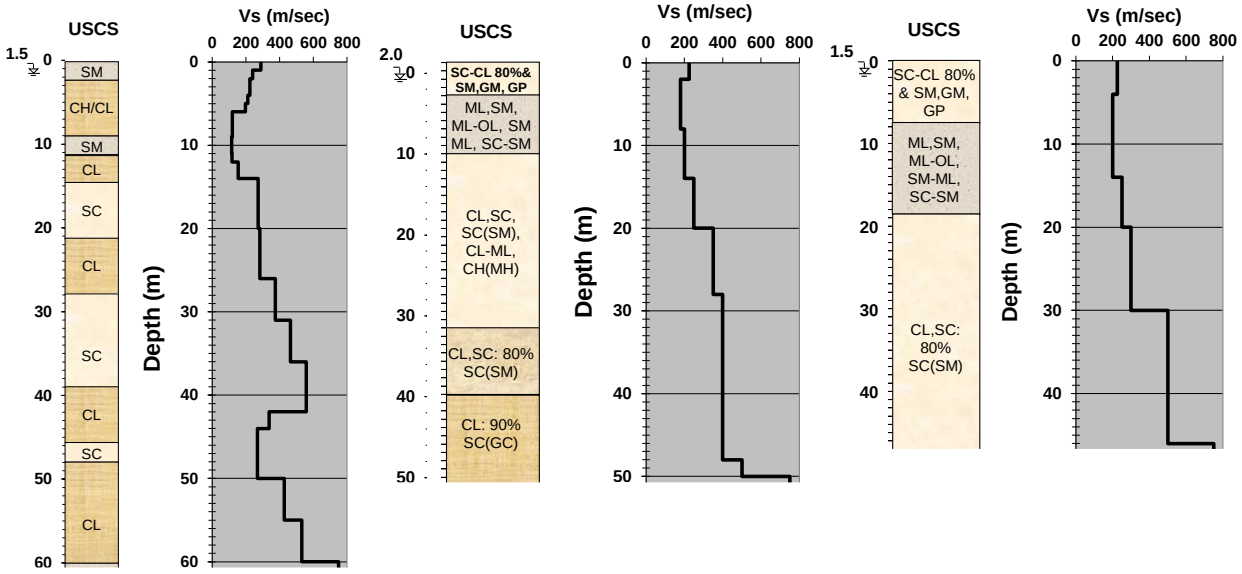

Fig. 2 – Schematic representation of the V_S profiles for sites SP1 (left), SP2 (middle) and SP3 (right) together with a general geotechnical characterization according to the USCS classification

2.2 Structural modelling

We conduct 2D numerical simulation of the reference building typology using the open-source computational platform OpenSees [10]. Inelastic force-based formulations are implemented for the two-dimensional with three degrees of freedom nonlinear beam-column frame element modelling, while the roof (trusses) of the building is modelled using "truss" elements (with two degrees of freedom). We use the uniaxial "*Steel01*" material to construct a uniaxial bilinear steel material object with kinematic hardening. The main parameters required, i.e. the yield strength (F_y), the initial elastic tangent (E_0) and the strain-hardening ratio (b), which is the ratio between post-yield tangent and initial elastic tangent, are taken equal to F_y = 235.0 MPa, $E_0 = 2.1 \cdot 10^5$ MPa and b=0.01 respectively. The nonlinear beam-column frame elements are subjected to both axial compression and bending, considering five Gauss-Lobatto [11] integration points along each member's length. The applied formulations allow both geometric nonlinearities (P-delta and large displacements/rotation effects) and material inelasticity to be captured. Distributed material inelasticity along the element is applied based on the fibre approach to represent the cross-sectional behaviour [12]. Each fibre is associated with a uniaxial

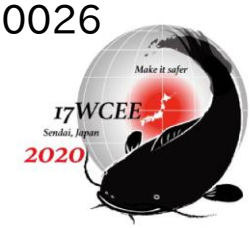

stress-strain relationship; the sectional stress-strain state of the beam-column elements is obtained through the integration of the nonlinear uniaxial stress-strain response of the individual fibres in which the section is subdivided. The truss elements are subjected only to axial compression. As they are constructed with a uniaxial material object, they consider strain-rate effects. The masses are applied as distributed along columns and beams (by assigning the specific weight of steel material) plus concentrated vertical loads on joints due to the existence of trusses on the normal direction.

2.3 Soil modelling

Each soil profile comprises several layers of cohesive and cohesionless soil material. The groundwater table is located at a depth of 1.5m, 2.0m and 1.5m for the soil profiles SP1, SP2, and SP3, respectively (Fig. 2). Saturated unit weights are used for the soil below this level and effective stress analysis is conducted using nine-node quadrilateral elements with both displacement and pore pressure degrees of freedom. Such elements are able to simulate fluid-solid coupling during the earthquake excitation, based on Biot's theory of porous medium [13]. In particular, the corner nodes of a nine-node element have three degrees of freedom, two translational and one pore pressure, while the interior nodes have only two translational degrees of freedom. To account for the finite rigidity of the underlying bedrock, a Lysmer-Kuhlemeyer [14] dashpot is incorporated at the base of the soil profile using a bedrock shear wave velocity of 627.0m/s, 750.0m/s and 750.0m/s for the soil profiles SP1, SP2 and SP3 respectively and a mass density of 2.2Mg/m^3. The Lysmer-Kuhlemeyer dashpot is assigned based on the viscous uniaxial material model and the 'zeroLength' element formulation at the same location, to connect the two previously defined dashpot nodes. This material model requires a dashpot coefficient that is defined according to Joyner and Chen [15] as the product of the mass density and shear wave velocity of the underlying bedrock including also the base area of the soil profile. To model the underlying elastic half-space necessitates that the nodes at the base of the soil model be left free to displace in the horizontal direction, be all given the same horizontal displacements and finally be fixed against vertical translation only. Mass and stiffness proportional Rayleigh damping is assigned to account for energy dissipation during seismic loading with a damping ratio equal to 2%. Periodic boundary conditions are used to ensure that free-field conditions exist at the horizontal boundaries of the model. In particular, the displacement degrees of freedom for the nodes on either side of the soil model are tied together imposing the same translational displacements in x and z directions, and rotation about the y-axis. Each soil profile is excited at the base by a horizontal force time history proportional to the known velocity of the ground motion [15]. Due to the consideration of an elastic half-space it was possible to directly apply the outcropping rock motion at the base of the soil model [16].

We employ a fully coupled (u-P) formulation, capable of simulating permanent shear-strain accumulation in clean medium-dense cohesionless soils during liquefaction and dilation due to increased cyclic shear stiffness and strength. The soil constitutive behaviour is based on the framework of multi-surface plasticity [17], with modifications by Yang [18]. The hardening law, the yield surface and the flow rule constitute the major components of the plasticity model. During the application of the gravity load, material behaviour is linear elastic. In the subsequent dynamic loading phase, the stress-strain response is elastic-plastic. To generate soil hysteretic response under cyclic loading, we adopt a purely deviatoric kinematic hardening rule [17]. This kinematic rule dictates that all yield surfaces may translate in stress space within the failure envelope [18-19] and be consistent with the Masing unloading/reloading criteria [20]. For the cohesionless soil layers, an elastic-plastic material, namely "PressureDependMultiYield02", is used in Opensees, where the yield function is assumed to follow the Drucker-Prager shape and the yield surface is a function of friction angle and cohesion. Plasticity is formulated based on the multi-surface concept, with a non-associative flow rule [18] that handles the soil contractive/dilative behaviour during shear loading to achieve appropriate interaction between shear and volumetric responses. For the cohesive soil layers, an elastic-plastic material in which plasticity exhibits only in the deviatoric stress-strain response, namely "PressureIndependMultiYield", is used. The volumetric stress-strain response is linear-elastic and is independent of the deviatoric response. This material is implemented to simulate monotonic or cyclic response of materials whose shear behaviour is insensitive to the confinement change. The yield function is assumed to follow the Von Mises shape and the yield surface is a function solely of undrained shear strength. Plasticity is formulated based on the multi-surface

concept, with an associative flow rule in which the incremental plastic strain vector is normal to the yield surface.

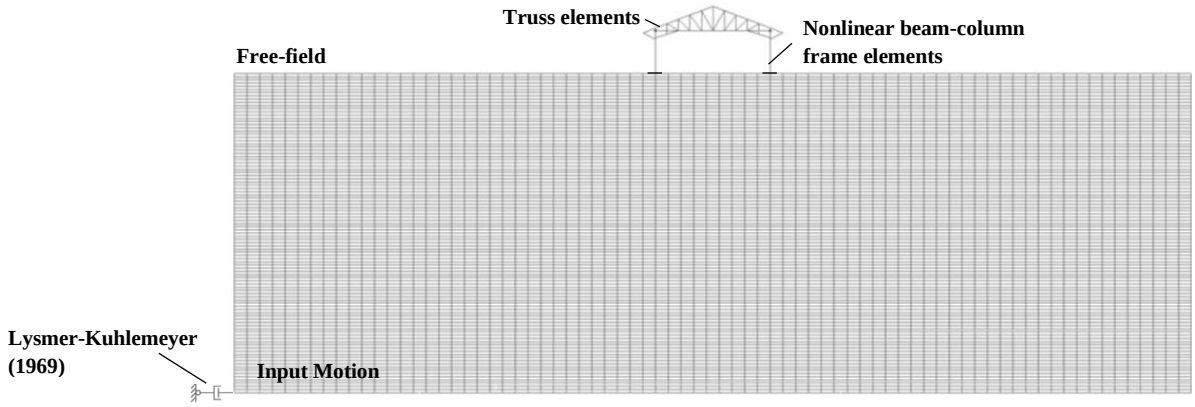

Fig. 3 – Finite element 2D model for the typical steel light-frame warehouse on liquefiable soil

2.4 Soil-structure interaction modelling

We apply the direct one-step approach, which accounts simultaneously for inertial and kinematic interaction schemes. Fig. 3 represents the 2D coupled finite element (FE) soil-structure model for the warehouse resting on liquefiable soil, which is subjected to combined ground shaking and liquefaction. The grids adopted for the different soils SP1, SP2 and SP3 have total lengths three times their depth to avoid spurious wave reflections at the vertical boundaries. Their dimensions are defined equal to 60.0m x 180.0m, 50.0m x 150.0m and 46.0m x 138.0m, respectively. Dense discretization is achieved using quadrilateral elements of 0.5m x 2.0m, considering that the maximum frequency of interest is set to 10Hz. This mesh allows an adequate number of elements to fit within the shortest wavelength of the propagating shear wave. Full bond is assumed between the structure's foundation and the soil nodes. The soil and the structure nodes at the level of foundation have appropriate constrains in order to ensure equal displacements. Shallow, relatively flexible foundations are considered, modelled as elastic beam-column elements of infinite rigidity, which allow columns to move differentially and hence permitting the computation of structural deformation demand using a numerical approach. In this case, it is furthermore assumed that no interface has been considered between the structure and the foundation and that failure will take place on the structural elements of the building, while the structural integrity of the foundation itself will not be affected by the liquefaction induced deformation.

3. Numerical analysis

3.1 Seismic input motion

A representative set of fifteen real ground motion records (Table 1) is selected from the European Strong-Motion Database to perform nonlinear incremental dynamic analyses. They are all referring to rock type or stiff soils (ground types A and B according to EC8) with moment magnitude (M_w) and epicentral distance R that range between $5.5<M_w<6.5$ and $0<R<45$km respectively. The primary selection criterion is the average acceleration spectra of the set to match the corresponding 5% damped median plus 0.5 standard deviations spectrum defined based on the ground motion prediction equation (GMPE) proposed by Akkar and Bommer [21]. The optimization procedure is performed using REXEL software [22] that allows obtaining combinations of accelerograms, which on average are compatible to the reference spectrum. Fig. 4 shows the mean elastic response spectrum of the records in comparison with the corresponding median plus 0.5 standard deviations Akkar and Bommer [21] spectrum. As shown in the figure, a good match between the two spectra is achieved.

Table 1 – List of earthquake records used for the dynamic analyses

Record Name	Date	M_w	Fault Mechanism	Epicentral Distance [km]	PGA [m/s^2]	EC8 Site class	Waveform ID
Umbria Marche (aftershock)	6/10/1997	5.5	normal	5	1.838	A	651
Valnerina	19/9/1979	5.8	normal	5	1.510	A	242
SE of Tirana	9/1/1988	5.9	thrust	7	4.037	A	3802
Lazio Abruzzo (aftershock)	11/5/1984	5.5	normal	15	1.411	A	990
Valnerina	19/9/1979	5.8	normal	5	2.012	A	242
Kozani	13/5/1995	6.5	normal	17	2.039	A	6115
Friuli (aftershock)	15/9/1976	6.0	thrust	12	1.339	A	149
Umbria Marche	26/9/1997	5.7	normal	23	1.645	A	763
Friuli (aftershock)	15/91976	6.0	thrust	14	2.586	B	134
Patras	14/7/1993	5.6	strike slip	9	3.337	B	1932
Kalamata	13/9/1986	5.9	normal	11	2.670	B	414
Umbria Marche 2	26/9/1997	6.0	normal	11	5.138	B	594
Montenegro (aftershock)	24/5/1979	6.2	thrust	17	1.708	B	229
Kefallinia island	23/1/1992	5.6	thrust	14	2.223	B	6040
Ano Liosia	7/9/1999	6.0	normal	14	2.159	B	1714

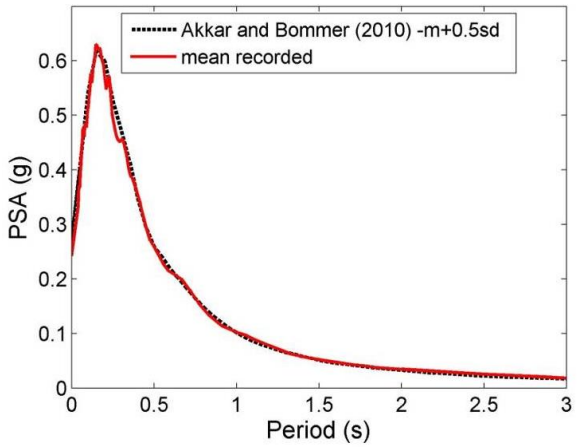

Fig. 4 – Average elastic response spectrum of the input motions in comparison with the corresponding median plus 0.5 standard deviations Akkar and Bommer [21] spectrum

3.2 Liquefaction identification

Layers of potential liquefaction are identified by the loss of effective confining stress (equal to zero) which is also verified by the corresponding stress-strain loops (e.g. at 7.0m below surface as shown in Fig. 5). Indicatively, Fig. 5 illustrates the computed variation of effective confinement with depth and stress-strain hysteresis loops at specific depth for one of the above input motions for SP2.

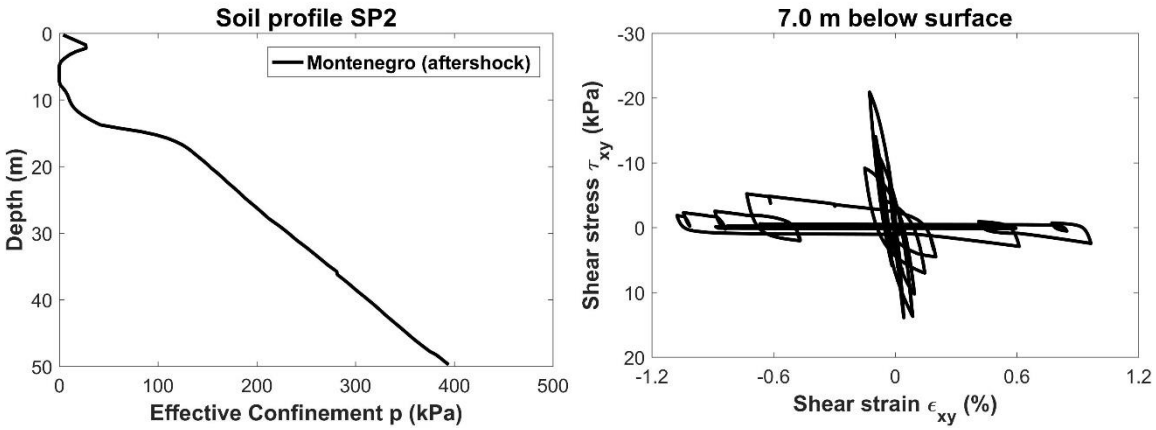

Fig. 5 – Variation of the effective confinement with depth (left) and stress-strain hysteresis loops at 7.0m depth (right) for the ID 229 input motion (Montenegro aftershock) for SP2

3.3 Incremental dynamic analysis

We conduct 2D IDA to estimate more thoroughly the seismic performance of the typical steel light-frame warehouse due to ground shaking and liquefaction. To express the scaling level an initial, temporary choice of IM is needed. Scaling can be re-expressed in any other scalable IM [23] after the runs are performed. In this study, the IM is initially described by the peak ground acceleration on rock outcropping conditions (PGA_{rock}). This IM is considered more appropriate due to its simplicity. Hence, IDA for the three SSI models is conducted by applying the 15 progressively scaled records, considering a first elastic run at 0.05g and an initial step of 0.1g, increased by a constant step of 0.1g, up to 0.8g. A sequence of at least ten runs is performed on each record, leading to a total of 450 dynamic analyses. The damage measure (DM) is expressed in terms of maximum inter-story drift (maxISD), which is known to relate well to dynamic instability and structural damage of frame buildings.

3.4 Efficiency of different seismic intensity measures

The selection of appropriate IMs is important for an accurate estimation of the consequences of combined ground shaking and liquefaction in the context of building performance. Knowledge and use of an efficient intensity measure (IM) will reduce variability and improve accuracy of the predicted measure of performance. The amplitude, frequency content and strong-motion duration are of engineering significance to characterize strong-motion recordings. Within this context, peak ground acceleration (PGA), peak ground velocity (PGV), Arias Intensity (I_a), Cumulative Absolute Velocity (CAV) and Average Spectral Acceleration ($S_{a,avg}$) can quantify the overall effects of above seismological parameters. In particular, PGA characterizes the earthquake ground motion peak amplitude (amplitude/intensity), PGV the intensity and frequency content of the earthquake motion, I_a and CAV the intensity and implicitly the duration of the ground motion and finally $S_{a,avg}$ is related to both the ground motion intensity and the frequency characteristics of the system. Arias Intensity (I_a) is defined as being proportional to the integral of the square of the acceleration history over the duration of the record, CAV is calculated as the integral of the absolute value of the acceleration time history over the full duration of the ground motion, while $S_{a,avg}$ is computed as the geometric mean of the spectral pseudo-acceleration ordinates over a certain range of periods for a 5% damping according to Bianchini et al. [24]. These ground-motion IMs are also capable of describing the damage potential of ground acceleration that lead to their efficient use in various engineering applications. Thus, the efficiency of the above IMs representing different aspects of the ground motion characteristics is examined to predict the seismic behaviour of typical steel light-frame warehouses considering liquefaction.

An efficient IM is identified through regression analyses correlating the different IMs and the numerically calculated EDP that relates to structural performance and damage potential (i.e. maximum inter-

story drift). More specifically, in all analysis cases we adopt a linear regression fit of the logarithms of the IM - maxISD data respectively which minimizes the regression residuals. It is noted that all the data from the three soil profiles are used for the construction of these relationships, as there are no large differences in the structural response (maxISD) calculated from the nonlinear dynamic analysis using the three soil profiles. Initially, the selected IMs refer to the input outcropping rock motion while appropriate IMs at surface are also investigated. The estimated dispersion sigma (σ) represents the conditional standard deviation of the regression (in natural log units) and is a metric of the efficiency of the IM with respect to the demand parameter (maxISD). Lower σ values yield less dispersion about the estimated median in the results indicating a more efficient IM. Fig. 6 presents comparative plots of the derived IM - maxISD relationships for quantifying the efficiency of the examined IMs at bedrock.

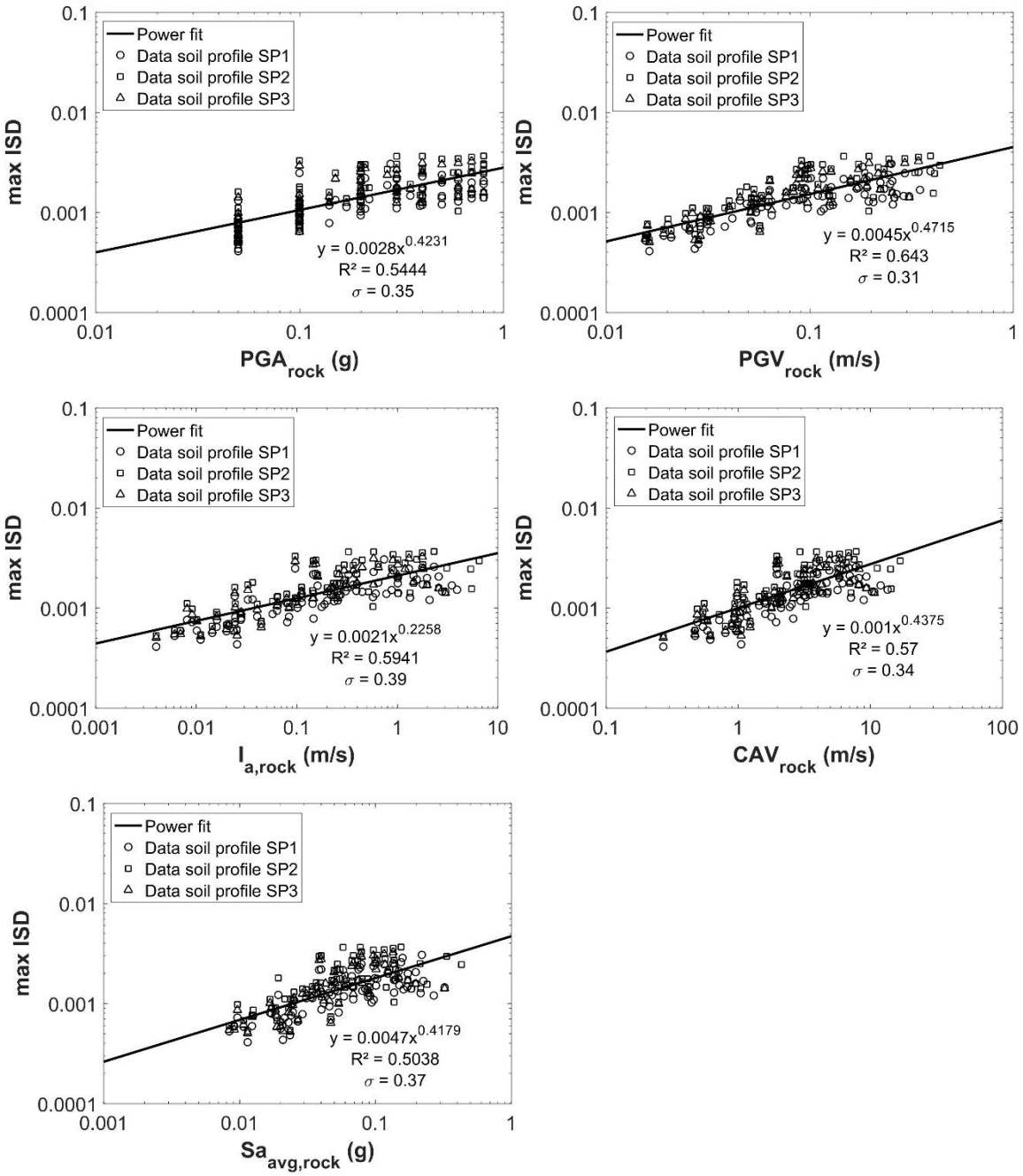

Fig. 6 – IM - maxISD relationships for quantifying the efficiency of the examined IMs at bedrock

It is noticed that the results in Fig. 6 show a relatively larger scatter for the I_a- maxISD pair compared to the other IM - maxISD pairs. Such difference could be attributed to the (lower) efficiency of the IM, i.e. I_a at rock, which is obvious from the highest sigma value used for the comparisons. It is also seen that the data display significantly less variability when considering PGV term in the regression, which seems to be the most efficient IM as it presents lower sigma values compared to the rest IMs. CAV and PGA generally display similar increased scatter (lower sigma values) with respect to PGV whereas $S_{a,avg}$ and I_a are the least efficient IMs. Based on the above considerations, PGV at rock is the most appropriate IM to assess the performance of steel light-frame port warehouses due to ground shaking and liquefaction.

To further investigate the efficiency of various IMs with respect to the demand parameter (maxISD) of the typical warehouse, appropriate IMs at surface are also statistically correlated with the numerically calculated maxISD. In particular, PGA and PGV at surface (PGA_{surf} and PGV_{surf} respectively) as well as the resulting permanent ground displacement vector induced by seismic soil failure due to liquefaction (PGD_{surf}) are examined as IMs. It is noted that the acceleration time histories imposed at the four footings of the structure are not the same, thus the maximum PGA, PGV and PGD imposed at the foundation level is considered. In addition, considering that the liquefaction-induced differential settlements become the major cause of damage to buildings [25-26], the maximum differential settlement at the foundation level caused by the combined effect of ground shaking and soil liquefaction is also examined as IM.

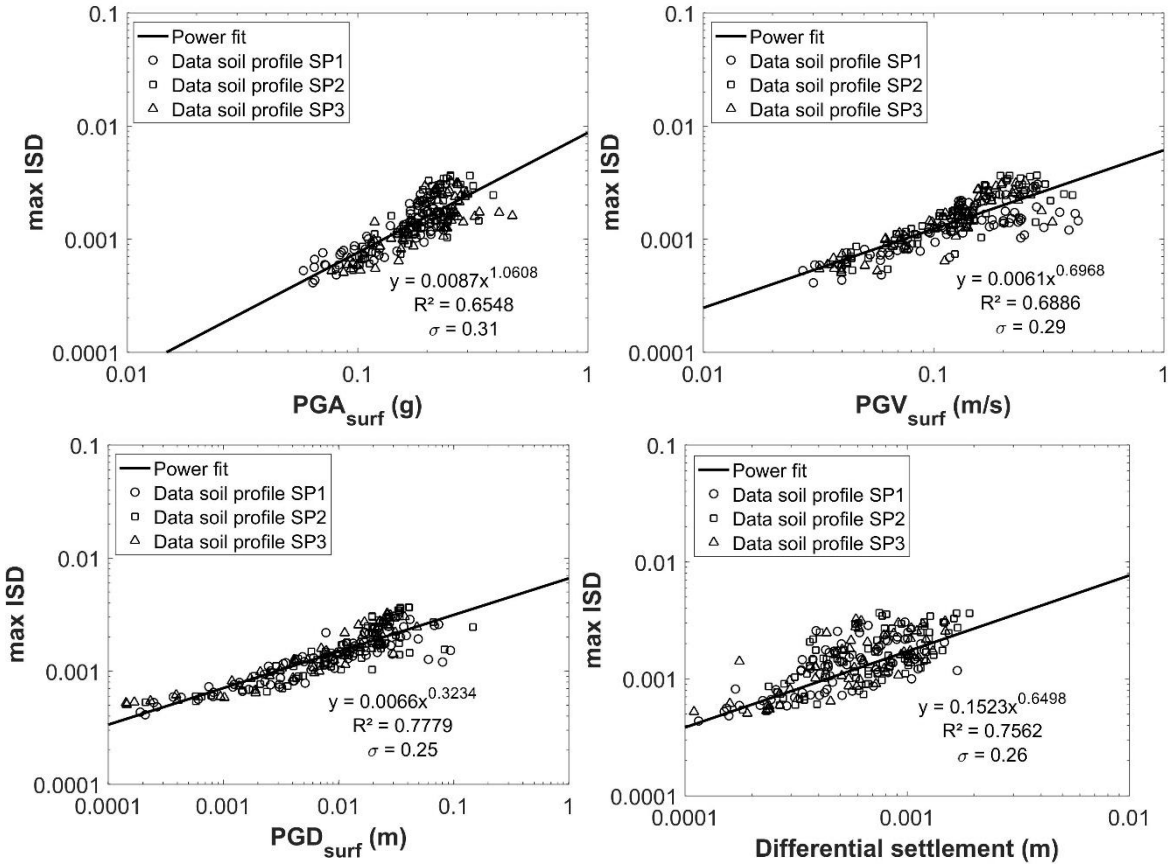

Fig. 7 – IM - maxISD relationships for quantifying the efficiency of the examined IMs at surface

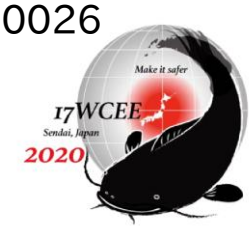

Fig. 7 illustrates the derived IM - maxISD relationships for quantifying the efficiency of the examined IMs at surface. In general, we observe lower sigma values and therefore IMs at surface are more efficient compared to the considered IMs at rock. This is due to the increased nonlinear behaviour of the soil introduced by the soil liquefaction, which may result in significant attenuation of the seismic motion at the ground surface and thus not such good correlation with structural damage. In addition, the results in Fig. 7 show a good correlation of both PGD_{surf} and differential settlement with the structural demand (maxISD) indicating that both IMs present low sigma values and therefore are more efficient compared to the other IMs at surface. PGV_{surf} follows next, while a relatively larger scatter is shown for the PGA_{surf} - maxISD pair.

4. Conclusions

Within the framework of this study, incremental dynamic analysis was performed for a typical port steel light-frame warehouse resting on liquefiable soils using a selected set of earthquake records. We implemented the direct one-step approach, where the soil and the structure are modelled and analysed as a single system, considering soil nonlinearity introduced by soil liquefaction. To identify efficient seismic IMs for the seismic assessment of these SSI systems considering liquefaction, we correlated various seismic IMs with the structural deformation demand (in terms of the maximum inter-story drift) through nonlinear regression analysis.

We concluded that the Peak Ground Velocity (PGV_{rock}) of the base excitation was found to better describe their performance followed by CAV_{rock} and PGA_{rock}. Moreover, we observed a good correlation of both PGD_{surf} and differential settlement at the foundation level with the structural demand (maxISD). Both IMs present lower sigma values compared to those referring to the input outcropping rock motion and therefore are more efficient compared to the considered IMs at rock. The results of this study can be used as the basis for the seismic vulnerability assessment of these type of buildings subjected to combined ground shaking and liquefaction. Overall, the use of an IM at rock is suggested when the local soil conditions are not known, while the usage of an IM at surface is justified for site-specific applications on critical buildings where adequate data from field measurements and/or detailed numerical analysis are available.

5. Acknowledgements

The research reported in this paper was carried out in the framework of the ‘‘Resilient, system-wide seismic risk assessment of port facilities. Application to Thessaloniki Port system’’ RESPORTS project (http://resports.gr/), funded by the Hellenic Foundation for Research and Innovation (HFRI) and General Secretariat for Research and Technology (GSRT) under Grant Agreement Number 754.

6. References

[1] Werner S (1998): Seismic guidelines for ports. Monograph no. 12. ASCE [Chapter 2].

[2] Pitilakis K, Crowley H, Kaynia A (Eds) (2014a): SYNER-G: Typology definition and fragility functions for physical elements at seismic risk. Buildings, lifelines, transportation networks and critical facilities. *Geotechnical, Geological and Earthquake Engineering*, **27**, Springer, Netherlands.

[3] International Navigation Association –PIANC (2001): *Seismic design guidelines for port structures*. Chairman: Iai S, Bakelma Publishers, Tokyo.

[4] National Institute of Building Sciences (2004): *Direct physical damage-general building stock*. HAZUS-MH Technical manual, Chapter 5. Washington, D.C.: Federal Emergency Management Agency.

[5] Ntaliakouras I, Pnevmatikos N (2017): Seismic vulnerability curves for industrial steel structures. *16th European Conference on Earthquake Engineering*, 18-21 June, Thessaloniki, Greece.

[6] Karafagka S, Fotopoulou S, Pitilakis K (2018): Vulnerability assessment of RC buildings and warehouses due to liquefaction displacements. *16th European Conference on Earthquake Engineering*, 18-21 June, Thessaloniki, Greece.

[7] Anastasiadis AJ, Raptakis DG, Pitilakis KD (2001): Thessaloniki's Detailed Microzoning: Subsurface Structure as basis for Site Response Analysis. *Pure and Applied Geophysics* – PAGEOPH, **158** (12):2597-2633, DOI: 10.1007/PL00001188.

[8] Pitilakis K, Argyroudis S, Fotopoulou S, Karafagka S, Kakderi K, Selva J (2018): Application of stress test concepts for port infrastructures against natural hazards. The case of Thessaloniki port in Greece. *Reliability Engineering & System Safety*, https://doi.org/10.1016/j.ress.2018.07.005.

[9] CEN (2004): EN 1998-5. Eurocode 8: *Design of structures for earthquake resistance - Part 5: Foundations, retaining structures and geotechnical aspects*. European Committee for Standardization, Brussels.

[10] Mazzoni S, McKenna F, Scott MH, Fenves GL (2009): Open system for earthquake engineering simulation user command-language manual. Berkeley, California: Pacific Earthquake Engineering Research Centre.

[11] Neuenhofer A, Filippou FC (1997): Evaluation of nonlinear frame finite-element models. *Journal of Structural Engineering*, ASCE, 123(7):958-966.

[12] Spacone E, Ciampi V, Filippou FC (1996): Mixed formulation of nonlinear beam finite element. *Computers & Structures*, 58(1):71-83.

[13] Biot MA (1962): Mechanics of deformation and acoustic propagation in porous media. *Journal of Applied Physics*, 33(4):1482-1498.

[14] Lysmer J, Kuhlemeyer AM (1969): Finite dynamic model for infinite media. *Journal of the Engineering Mechanics Division*, ASCE, 95:859-877.

[15] Joyner WB, Chen ATF (1975): Calculation of nonlinear ground response in earthquakes. *Bulletin of the Seismological Society of America*, 65(5):1315-1336.

[16] Kwok AOL, Stewart JP, Hashash YM, Matasovic N, Pyke R, Wang Z, Yang Z (2007): Use of exact solutions of wave propagation problems to guide implementation of nonlinear seismic ground response analysis procedures. *Journal of Geotechnical and Geoenvironmental Engineering*, ASCE, **133** (11):1385-1398.

[17] Prevost JH (1985): A simple plasticity theory for frictional cohesionless soils. *Soil Dynamics and Earthquake Engineering*, **4** (1):9-17.

[18] Yang Z (2000): *Numerical Modeling of Earthquake Site Response Including Dilation and Liquefaction*. PhD Thesis, Department of Civil Engineering and Engineering Mechanics, Columbia University, New York.

[19] Parra E (1996): *Numerical modelling of liquefaction and lateral ground deformation including cyclic mobility and dilation response in soil systems*. PhD thesis, Department of Civil Engineering, Rensselaer Polytechnic Institute, Troy, New York.

[20] Masing G (1926): Eigenspannungen and verfertigung beim messing. Proceedings of the 2nd International Congress for Applied Mechanics, Zurich, Switzerland

[21] Akkar S, Bommer JJ (2010): Empirical equations for the prediction of PGA, PGV and spectral accelerations in Europe, the Mediterranean and the Middle East. Seismological Research Letters, 81:195–206

[22] Iervolino I, Galasso C, Cosenza E (2010): REXEL: computer aided record selection for code-based seismic structural analysis. Bulletin of Earthquake Engineering, 8(2):339-362, https://doi.org/10.1007/s10518-009-9146-1.

[23] Vamvatsikos D, Cornell CA (2002): Incremental dynamic analysis. *Earthquake Engineering & Structural Dynamics*, **31**(3):491–514.

[24] Bianchini M, Diotallevi P, Baker JW (2009): Prediction of Inelastic Structural Response Using an Average of Spectral Accelerations. *10th International Conference on Structural Safety and Reliability* (ICOSSAR09), Osaka, Japan.

[25] Bird JF, Bommer JJ, Crowley H, Pinho R (2006): Modelling liquefaction-induced building damage in earthquake loss estimation. *Soil Dynamics and Earthquake Engineering*, **26** (1):15-30.

[26] Bird JF, Crowley H, Pinho R, Bommer JJ (2005): Assessment of building response to liquefaction-induced differential ground deformation. Bulletin of the New Zealand National Society for Earthquake Engineering, **38** (4):215-34.

